Int. J. Electrochem. Sci., 12 **(2017)** 4640 – 4653, doi: 10.20964/2017.06.19

International Journal of
ELECTROCHEMICAL
SCIENCE
www.electrochemsci.org

Improving the Cycling Performance and Thermal Stability of $LiNi_{0.6}Co_{0.2}Mn_{0.2}O_2$ Cathode Materials by Nb-doping and Surface Modification

Haruki Kaneda[*], *Yuki Koshika, Takuma Nakamura, Hiroaki Nagata, Ryozo Ushio, Kensaku Mori*

Sumitomo Metal Mining Co., Ltd., Battery Research Laboratories, 17-3, Isoura-cho, Nihama, Ehime, 792-0008, Japan
[*]E-mail: Haruki_Kaneda@ni.smm.co.jp

Received: 6 January 2017 / *Accepted:* 23 March 2017 / *Published:* 12 May 2017

Niobium (Nb)-doped, Li_3NbO_4 surface-modified $LiNi_{0.6}Co_{0.2}Mn_{0.2}O_2$ (NCM622) cathodes were prepared using solid-phase reactions. These modifications helped in improving the thermal stability and cycling performance of the cathodes. XRD and EDX measurements of the prepared samples confirmed the uniform distribution of Nb, whereas Li_3NbO_4 was found to occur at the grain boundaries and on the surface of primary NCM622 particles. The thermal stability of the prepared samples was evaluated by measuring the amount of O_2 released from the cathode material during overcharging. This quantification was conducted using a gas chromatography–mass spectroscopy analysis. Decomposition of the NCM622 cathode material was suppressed by Nb-doping. Furthermore, electrochemical tests showed that the Nb-doped, Li_3NbO_4 surface-modified NCM622 exhibited an excellent cycling performance over 500 cycles in the 3.0–4.1 V voltage range at a current rate of 2 C at 60 °C, during which the sample retained 91.4% of its initial capacity. This capacity retention was much higher than that for both the samples prepared using only Nb doping without Li_3NbO_4 surface modification (36.8%) and that of undoped NCM622 (70.7%). Our results indicate that Nb doping and Li_3NbO_4 surface modification are effective for improving the cathode's thermal stability and cycling performance, respectively.

Keywords: Lithium-ion battery, NCM622 cathode material, Nb-doping and Li_3NbO_4 surface modification, cycling performance, thermal stability

1. INTRODUCTION

Lithium-ion batteries (LIBs) are popular power sources, particularly for portable electronic devices, because of their excellent electrochemical performance, including high energy density, high voltage, and a long life cycle [1,2]. In recent years, LIBs have been widely used in plug-in hybrid

vehicles (PHEV) and electric vehicles (EV) [3]. The employed LIBs in these vehicles are required to possess a high energy density, durability, and good thermal stability. In addition, the low production costs of LIBs make them feasible for use in large-scale projects. Considering the aforementioned requirements for LIBs, Ni-rich layered cathode materials have proven to be promising. $LiNi_{0.6}Co_{0.2}Mn_{0.2}O_2$ (NCM622) [4] in particular is interesting owing to both its substantial energy capacity and cost, which is lower than that of the currently used commercial materials such as $LiNi_{1/3}Co_{1/3}Mn_{1/3}O_2$ and $LiNi_{0.5}Co_{0.2}Mn_{0.3}O_2$. However, NCM622 suffers from a number of issues such as a poor cycling performance and thermal instability; the poor cycling performance is believed to be due to cation mixing [5,6], whereas the thermal instability seems to be due to its unstable crystal structure when overcharging [7].

Several strategies have been proposed for overcoming these problems; for instance, to improve the cycling performance of Ni-rich layered cathode materials, it is necessary to stabilize the crystal structure and suppress the surface degradation of the cathode. To this end, studies have attempted to modify the surface using coatings made of materials such as metal oxides [8–11], metal phosphates [12], and metal fluorides [13]. These coatings are able to prevent undesirable reactions occurring between cathode materials and an electrolyte. Recently, ionic conductive materials containing a large amount of lithium have attracted attention for use as coating materials because they not only act as a protective layer but also create Li^+ insertion sites and can be used as lithium storage materials; for example, it has been reported that lithium-ion conductive materials such as $Li_2O–2B_2O_3$ glass and Li_2SiO_3 effectively improve the electrochemical performance because of the high conductivity of Li^+ ions [14–16].

Several studies have also investigated how the thermal stability of cathodes can be improved through metal doping using, for example, Ti [17], Al [18], and core-shell materials [19]. We will focus on investigating high-valent metal candidates. It has been reported that high-valent metals, e.g., Mo, are effective for suppressing the changes that may occur in the structure of a crystal because of heating and can inhibit the release of O_2 during the changes triggered by heating during overcharging [20]. Nb is also a high-valent metal that has been found to form strong Nb–O bonds [21,22]. The introduction of a strong Nb–O bond into the layered structure of cathodes is therefore expected to improve their thermal stability. Furthermore, Nb has been found to form Li–Nb–O compounds, and these possess high conductivity owing to the Li^+ ions [23,24]. Therefore, we anticipate that Li–Nb–O compounds will prove very useful in the modification of the surfaces of cathode materials and ultimately improve the cycling performance of cathodes.

Based on these findings, we consider that using Nb for the modification of the bulk structure as well as that of the surface of cathode materials will be an effective way to simultaneously improve both the cycling performance and the thermal stability of these cathodes. Some previous studies have found the co-modification of bulk and surface of cathode materials to be effective in improving a cathode's electrochemical performance [25,26]; however, very few studies have reported on the simultaneous improvement of the cycling performance and thermal stability. Moreover, the modification of bulk structures and surface of cathode materials often involves complicated processes, such as the citrate precursor method [25] and the chemical oxidation polymerization method [26],

which are difficult to use at industrial scales. Therefore, it is necessary to synthesize our cathode materials using a simple method that could be readily used at an industrial scale.

In this study, we attempt to modify both the bulk structure and the surface of cathode materials using a simple method; our aim is to improve the thermal stability and cycling performance of Ni-rich cathode materials. To this end, we prepared Nb-doped and Li_3NbO_4 surface-modified NCM622 cathode materials using only a solid-phase reaction and investigated their resulting structures, element distribution, thermal stability, and electrochemical performance.

2. EXPERIMENTAL

2.1. Synthesis of the Nb-doped and Li_3NbO_4-surface-modified $LiNi_{0.6}Co_{0.2}Mn_{0.2}O_2$ cathodes

The $(Ni_{0.6}Co_{0.2}Mn_{0.2})(OH)_2$ precursors were synthesized using a co-precipitation method. In a nitrogen environment, an aqueous solution of $NiSO_4 \cdot 6H_2O$, $CoSO_4 \cdot 7H_2O$, and $MnSO_4 \cdot H_2O$ (Ni:Co:Mn = 6:2:2 molar ratio) with a total concentration of 2.0 mol L^{-1} was added into a continuously stirred tank reactor. To control the pH level of the solution, a 25 wt% NaOH aqueous solution was added to the reactor and a 25 wt% NH_4OH aqueous solution was used as a chelating agent. The pH level was adjusted to 11.8, and the temperature was set to 45 °C. Once the reaction was complete, the $(Ni_{0.6}Co_{0.2}Mn_{0.2})(OH)_2$ precursors were filtered, washed by a NaOH aqueous solution in which purified water was used, and dried for 24 h at 120 °C in a dryer. The prepared precursors, i.e., a Li_2CO_3 powder, and a dry-milled Nb_2O_5 powder (Wako, Japan) were thoroughly mixed in a ratio of Li/(Ni + Mn + Co + Nb) = 1.03 (Nb = 0, 1.0, and 3.0 mol%). The cathode samples in this study were synthesized using a solid-phase reaction. The mixture was pre-heated at 700 °C for 2 h and then sintered for 10 h at 900 °C in an O_2-filled furnace. The prepared Nb = 0, 1.0, and 3.0 mol% doped NCM622 cathode materials were named Nb-0, Nb-1, and Nb-3, respectively.

2.2. Characterization

The crystalline phases of the prepared samples were identified using X- ray powder diffraction (XRD) (X'Pert Pro MPD, PANalytical, the Netherlands) that uses Cu Kα radiation at 45 kV and 40 mA. Refinements as per the Rietveld method were performed using the X'Pert HighScore Plus software (PANalytical, the Netherlands). The cross-sectional microstructure and elemental distribution of the prepared samples were examined using scanning transmission electron microscopy (STEM, HD-2300A Hitachi, Japan) aided by an energy-dispersive X-ray (EDX) detector (GENESIS, EDAX, Japan).

The electrochemical properties of the samples were characterized using laminate cells (50 × 30 mm) that were assembled in an Ar-filled glove box at a dew point of −60 °C. The prepared samples, described in section 2.1, were applied to the cathode's surface, whereas artificial graphite was used for the anode and 1.0 M $LiPF_6$ in a 3:7 vol% mixture of ethylene carbonate (EC)/diethyl carbonate (DEC) electrolyte and polyethylene (PE) separators were employed. The cathode was prepared by coating an

Al laminate with a slurry mixture that contained 85 wt% of the prepared cathode materials and 10 wt% carbon black (which was used as a conducting agent); the remaining 5 wt% was a binder material that comprised polyvinylidene fluoride (PVdF) dissolved in *N*-methyl-2-pyrrolidone (NMP). The cathodic electrodes were roll-pressed at a liner pressure of 153 N mm^{-1} and then dried for 8 h at 120 °C in a vacuum. After drying, the electrolyte was poured into the cell, which was sealed with the Al laminate. The laminate cells were then cycled at a voltage range of 3.0–4.1 V at a current rate of 2 C at 60 °C. After the cycling tests, the laminate cells were disassembled and the electrodes were removed from the cells and washed with dimethyl carbonate (DMC) before being dried. An XRD measurement was performed on the cathode electrodes both before and after the cycling tests. Furthermore, the cathode electrodes, both before and after the cycling tests, were dissolved in diluted nitric acid, and inductively coupled plasma-mass spectroscopy (ICP-MS) was used to quantify the amount of transition metals and Nb on the cathode electrodes. The ratio of residual metals in the cathode materials was obtained from the amount of metal before and after the cycling tests.

The O_2 gas released from the cathode materials during overcharging was evaluated using gas chromatography–mass spectroscopy analysis (GC–MS, QP-2010plus, Shimadzu, Japan), which indicated the thermal stability of the samples. The prepared cathode materials were overcharged at 4.5 V using a constant current charge rate of 0.2 C. After the overcharged state was reached, the electrodes were removed from the cells, washed with DMC, and then dried. Approximately 2.0 mg of the overcharged cathode materials were then loaded into a column. The column was set in a specimen holder filled with He, which acted as a carrier gas during heating. The cathode material was heated from room temperature to 450 °C at a rate of 10 °C min^{-1}. The O_2 gas released from the cathode material was quantified using GC–MS.

3. RESULTS AND DISCUSSION

3-1. XRD and STEM-EDX

Figure 1 shows the XRD patterns of the prepared samples. All the samples exhibited well-defined layer structures based on a hexagonal α-$NaFeO_2$ structure with an R3m space-group. For Nb-3, the Li_3NbO_4 (ICDD card No. 75-902) peak was observed at 2θ = 25.9° and 42.9°. Table 1 shows the lattice constants and the I(003)/I(104) ratios of the prepared samples. The lattice constants a and c increased as the amount of Nb-doping increased because the diameter of Nb^{5+} (0.64 Å) is larger than those of Ni^{3+} (0.56 Å), Co^{3+} (0.545 Å), and Mn^{4+} (0.53 Å) [27]; this indicates that the Nb solid dissolved into the NCM622 lattice. Because the amount of Nb-doping of NCM622 exceeded the solid-solubility limit for the Nb-3 sample, we consider that Nb reacted with excess Li and formed Li_3NbO_4. The I(003)/I(104) peak intensity ratio can be used as a parameter for evaluating the extent of cation mixing within the structure [5]; cation mixing is related to a cathode material's electrochemical characteristics. In general, a I(003)/I(104) ratio of 1.2 or above indicates good cation ordering [28]. For this parameter, our samples exhibited values that were greater than 1.2, which indicated that good cation ordering was obtained for all of the samples.

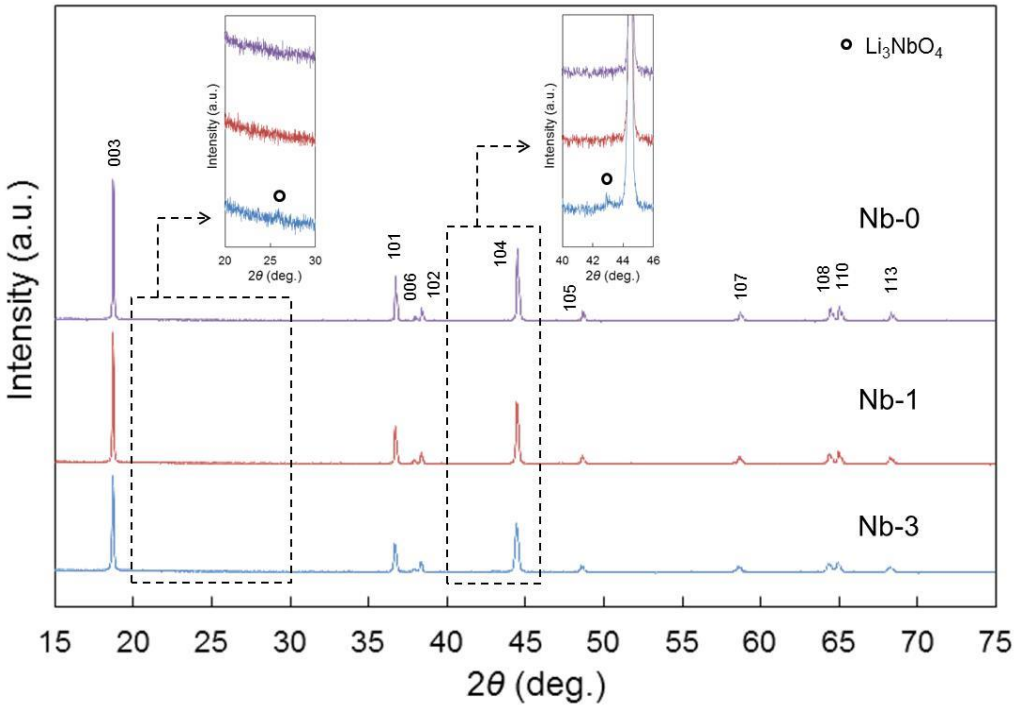

Figure 1. XRD patterns for the prepared Nb-0, Nb-1, and Nb-3 samples.

Table 1. Lattice constants and I(003)/I(104) ratios of the prepared Nb-0, Nb-1, and Nb-3 samples.

Sample	a (Å)	c (Å)	I(003)/I(104)
Nb-0	2.8658	14.2128	1.55
Nb-1	2.8678	14.2286	1.76
Nb-3	2.8706	14.2397	1.80

Figure 2 shows the STEM images and the EDX mappings of Nb-1 and Nb-3. Ni, Co, and Mn were uniformly distributed in all of the samples, which indicates that Nb was doped into the lattice in both Nb-1 and Nb-3. These results agree with the XRD results presented in Table 1. For Nb-1, the result of EDX line scan shows that Nb doping had a uniform profile. The Nb-3 sample, however, exhibited a different result; the dotted red area in the EDX line scan of Nb-3 highlights the region where the concentrations of Ni, Co, and Mn were lower than that of Nb. This result indicates that the Nb in Nb-3 was not only doped into the lattice but was also highly concentrated at the grain boundaries and at the cathode's surface. Using the XRD results, we found that Li_3NbO_4 formed at the grain boundaries and on the surface of the cathode material.

From the above results, we can conclude that Nb-doped NCM622 (Nb-1) and Nb-doped, Li_3NbO_4 surface-modified NCM622 (Nb-3) can both be prepared using a solid-phase reaction.

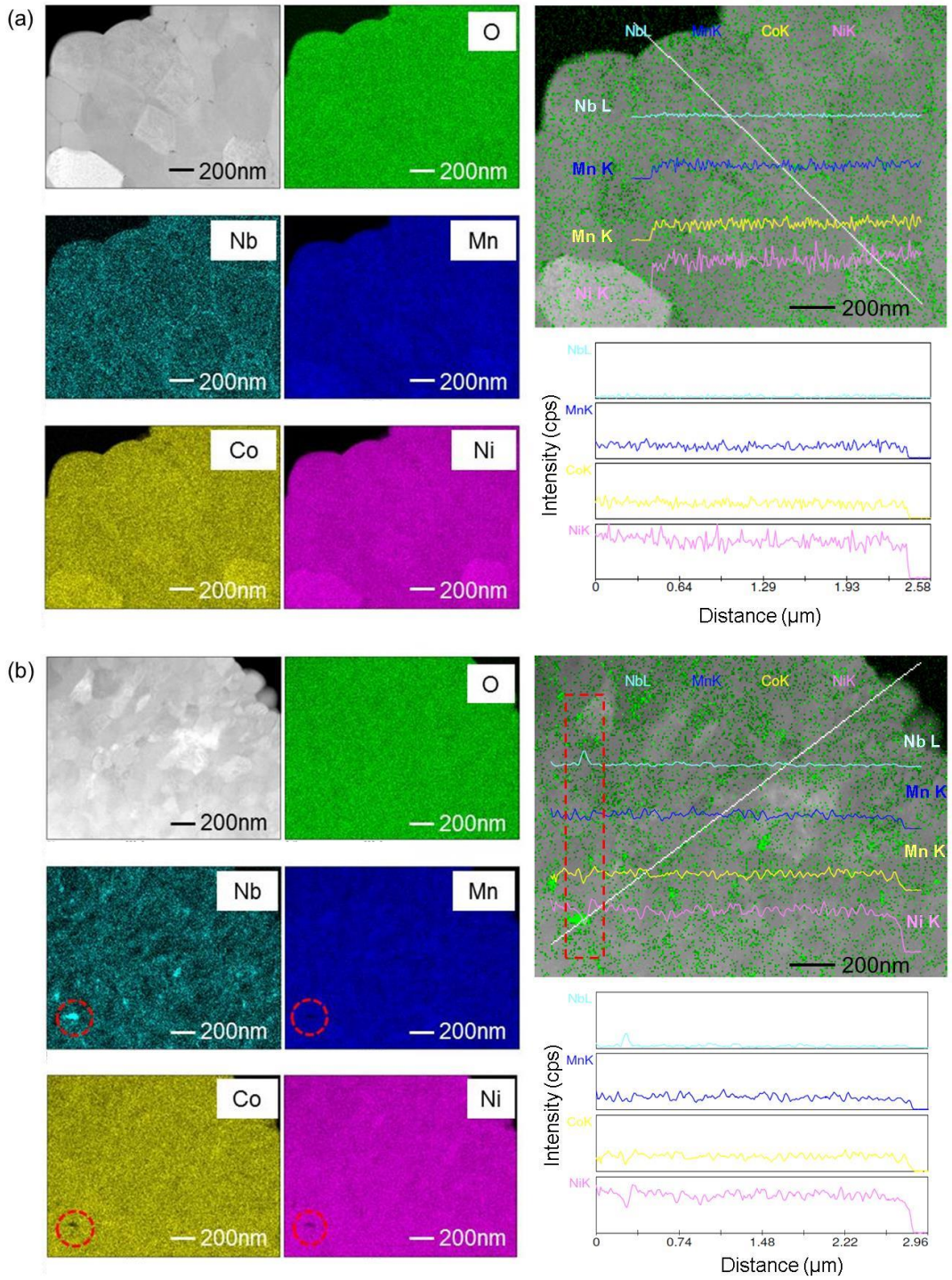

Figure 2. STEM images and EDX results for (a) Nb-1 and (b) Nb-3. The dotted red circles correspond to areas with high Nb concentrations.

3.2. Evaluation of Thermal Stability

To investigate the thermal stability of the prepared samples, we performed quantitative measurements of the O_2 released during the overcharging of the cathode materials using GC–MS analysis.

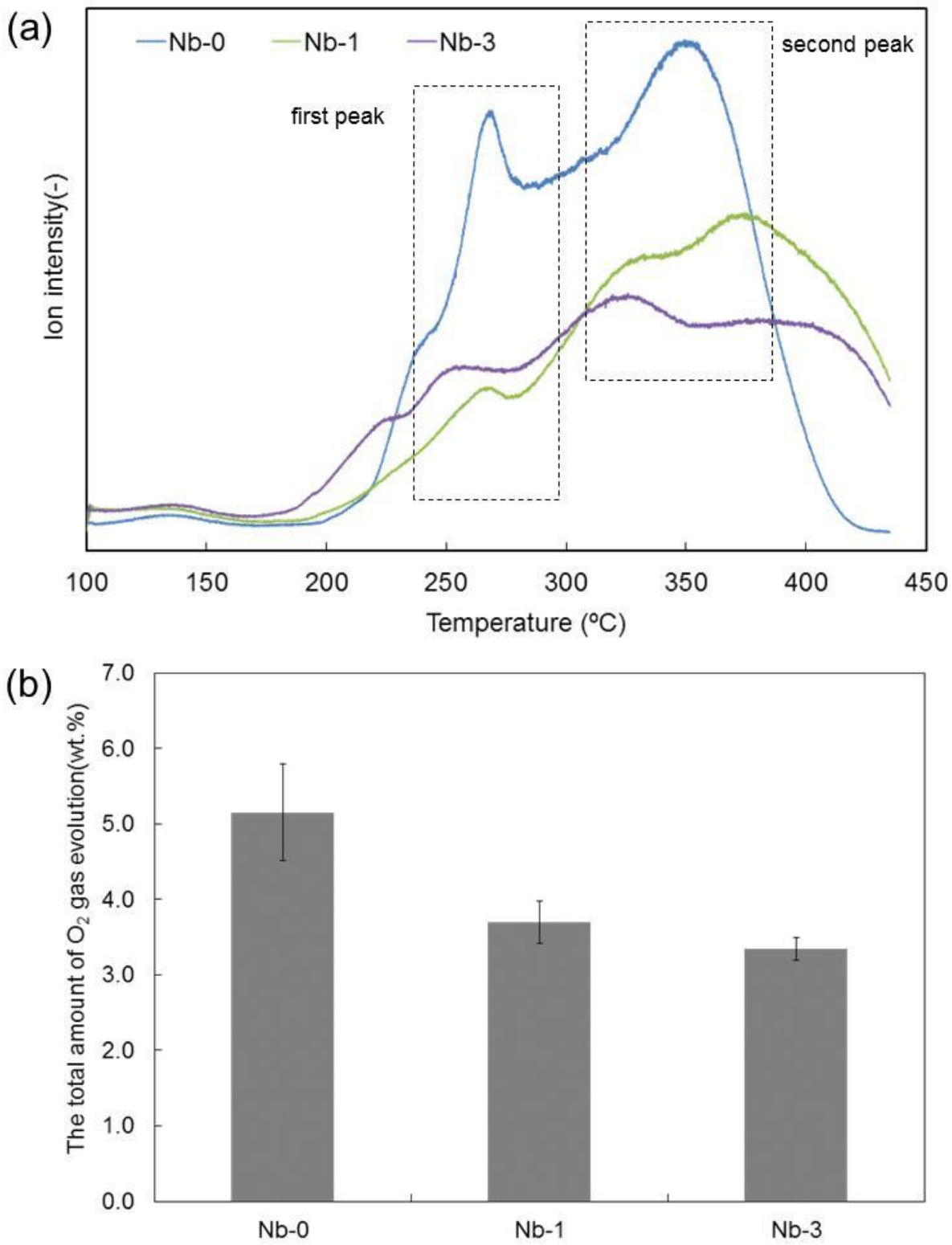

Figure 3. (a) GC–MS spectra and (b) the total amount of O_2 released from Nb-0, Nb-1, and Nb-3 when the samples were overcharged at 4.5 V.

The release of O_2 gas (m/z = 32) is reported to be closely related to the phase transitions that occur during the thermal decomposition of cathodic materials [29,30]; thus, by evaluating the amount of O_2 released during such conditions, the thermal stability of a cathodic material can be evaluated,

albeit indirectly. Figure 3 shows the GC–MS spectra and the total amount of O_2 released for the overcharged samples at 4.5 V. The first peak can be seen to be formed at 230–300 °C and the second peak at 300–390 °C; these correlate with the phase transitions from the layered to the spinel phase and from the spinel to the rock-salt phase, respectively. In Nb-0, the onset temperature of the O_2 release was approximately 200 °C and there was a sharp O_2 release peak between 250 and 270 °C. A second O_2 release peak was observed between 300 and 370 °C, and Nb-0 completely transformed to the rock-salt phase at approximately 420 °C.

The peak profile and the total amount of O_2 released by the Nb-doped samples were noticeably different from those of Nb-0. The first and second peaks that were observed for Nb-1 and Nb-3 were much smaller than those of Nb-0; i.e., the Nb-doped samples slowly released O_2 and the total amount of O_2 was therefore lower than that calculated for the Nb-0 sample. This result indicates that Nb doping aided in suppressing the structural changes and O_2 release that typically occur during overcharging. It has been suggested that Nb forms Nb–O bonds in the Nb-doped samples. According to a study on bond dissociation energy, the order of metal-oxygen bonding strengths is assumed to be Nb–O (753 kJ mol^{-1}) > Mn–O (402 kJ mol^{-1}) > Ni–O (391.6 kJ mol^{-1}) > Co–O (368 kJ mol^{-1}) [22]. Thus, Nb bonds strongly with oxygen in the cathode materials and is therefore believed to contribute to suppressing the release of O_2 caused by the heating that occurs during overcharging. In addition, there is a possibility that Nb suppresses the phase transitions caused by this heating; Konishi *et al.*, for example, have reported a high-valence element named Mo^{6+}, which is effective in suppressing the structural change from the spinel phase to the rock-salt phase [20]. In our results, the second peak (roughly at 300–390 °C), which corresponded with the phase transition from the spinel to the rock-salt phase, was lower than that reported by Konishi *et al.*; this indicates that Nb suppressed the structural changes in the cathode materials.

Based on the above findings, we concluded that doping the crystal structure of NCM622 with Nb was effective for improving the Ni-rich cathode's thermal stability.

3.3. Electrochemical Properties

Figure 4 highlights the cycling performance of the prepared samples between 3.0 and 4.1 V and at a current rate of 2 C at 60 °C. Although Nb-0 retained 70.7% of its initial discharge capacity after 500 cycles, Nb-3 was found to have a capacity retention of 91.4%. Nb-1 had the worst capacity retention (36.8%). According to a previous study, when cycling in a voltage range of 3.0–4.3V at a current rate of 1 C at 55 °C, the Nb doping of $Li(Ni_{0.5}Co_{0.2}Mn_{0.3})_{0.99}Nb_{0.01}O_2$ exhibits a good capacity retention compared with $LiNi_{0.5}Co_{0.2}Mn_{0.3}O_2$ without Nb-doping after 100 cycles [31]; In the present study, Nb-1 was found to have the highest capacity retention at up to 100 cycles, which was similar to the results of previous studies. However, the Nb-1 sample in the present study rapidly degraded after approximately 200 cycles, which indicates that Nb-1 degraded even though the other samples did not.

To investigate the differences between the samples' cycling capacity retention, the cycling performances of the prepared samples were investigated using electrochemical impedance spectroscopy (EIS) and XRD measurements. Moreover, the ratio of the residual metals in the cathode

materials after the cycling tests was analyzed to confirm if the transition metals or/and Nb had been dissolved from the cathode materials during the cycling tests.

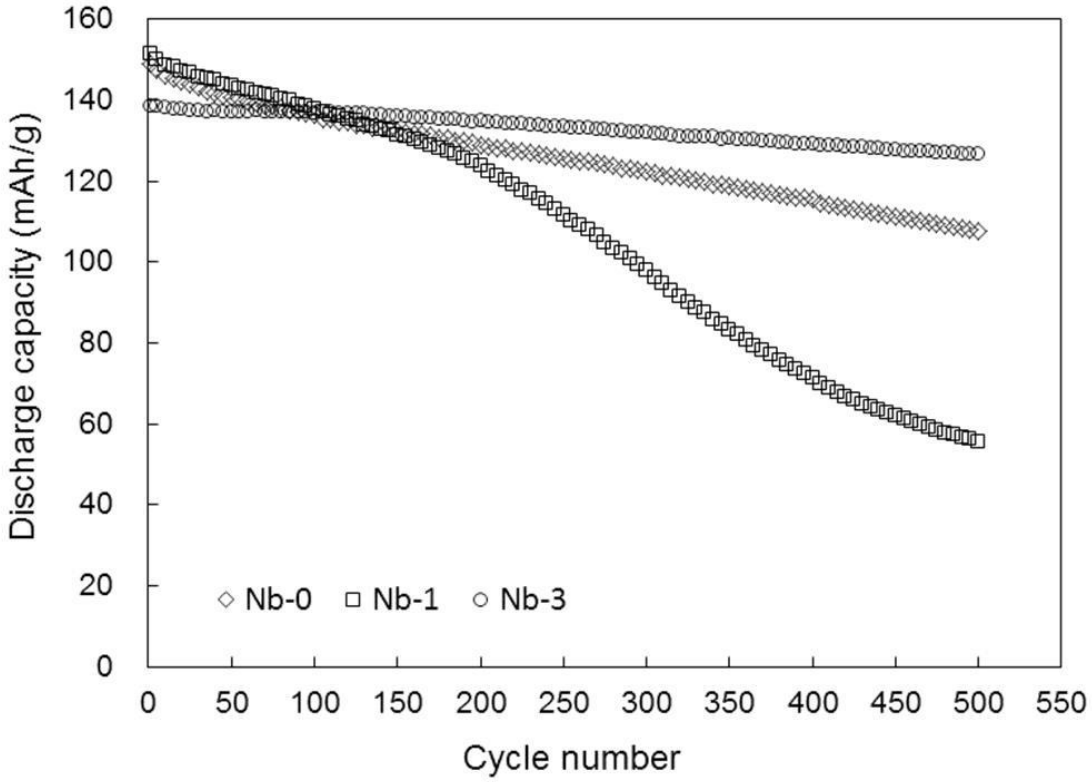

Figure 4. Cycling performance of the prepared samples in the 3.0–4.1 V voltage range and at a current rate of 2 C at 60 °C.

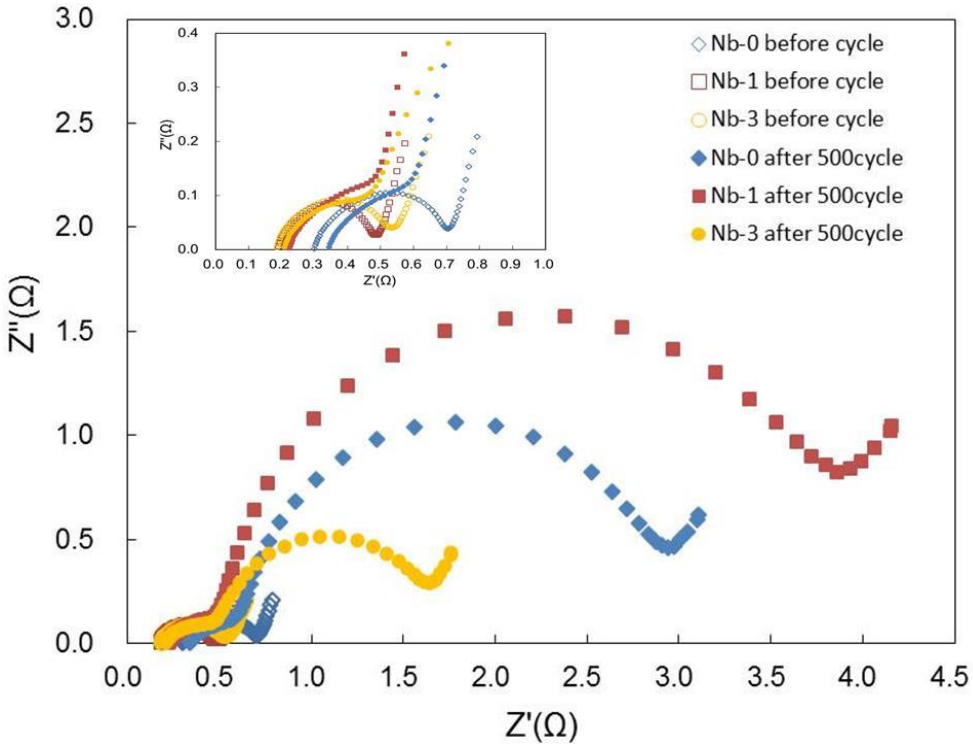

Figure 5. Impedance spectra of the prepared samples before and after the cycling tests at 3.9 V.

Figure 5 shows the impedance spectra of Nb-0, Nb-1, and Nb-3 both before and after the cycling tests were conducted at 3.9 V. The impedance spectra for each of the samples show two semi-circles in the high- and intermediate-frequency ranges, along with a sloping line in the low-frequency range. The second semicircle is considered to correspond with the charge-transfer resistance (R_{ct}) of Li^+ ion migration through the cathode surface–electrolyte interface, which has been outlined by a previous study [32]. As shown in Fig. 5, the R_{ct} of all of the samples was roughly similar before the cycling tests; however, the R_{ct} of Nb-3 (1.35 Ω) was much lower than those of Nb-0 (2.26 Ω) and Nb-1 (3.57 Ω) after the cycling tests. This increase in R_{ct} during the cycling tests is a significant indicator of interface degradation between the cathode materials and the electrolyte used owing to undesirable side reactions [33]. The EIS results indicate that the cathode surface of Nb-3 degraded only slightly, whereas that of Nb-1 degraded drastically.

The stability of the structure of the cathode materials after the cycling tests was also investigated. Figure 6 shows the XRD patterns of the prepared samples both before and after the cycling tests. The XRD patterns of all of the samples after the cycling tests were different from those before the tests; in particular, the (003) and (006) peaks shifted toward lower angles, whereas the (104) and (101) peaks shifted toward higher angles in Nb-0 and Nb-1, respectively. These peak shifts are related to changes in the crystal structure [34,35]. Since the peak shift of Nb-1 was the largest when compared with those of the other two samples, the structural damage to Nb-1 was the most serious after the cycling tests. The XRD pattern of Nb-3, meanwhile, changed only slightly after the tests. More interestingly, Li_3NbO_4 was observed in the case of Nb-3 even after the cycling tests, which indicates that Li_3NbO_4 has high chemical stability. Therefore, the surface of Nb-3 as well its bulk structure was found to not degrade after the tests.

Table 2 shows the ratio of the residual metals in the cathode materials after the cycling tests. As shown in Table 2, the amounts of Ni, Co, and Mn were the same both before and after the cycling tests; this indicates that they did not dissolve in the cathode materials in all of the samples we tested. Thus, in this study, the dissolution of the transition metals from the cathode materials was not the main factor contributing to cathode degradation. However, Nb dissolved in the cathode materials in the Nb-doped samples, and the amount of Nb that dissolved in Nb-1 was larger than that dissolved in Nb-3. In general, during the cycling tests, the cathode materials were entirely exposed to the electrolyte, which meant that the materials could have been continuously eroded by the HF that formed during the decomposition of electrolyte. Consequently, the performance of the cathode slowly degraded [36]. In the Nb-1 sample, the reaction with HF was gentle, similar to the case of the other samples during the initial stage of the cycling tests; however, we presume that HF specifically reacted with the Nb in the crystal structure of the cathode as the number of cycles increased. Thus, it is suggested that Nb-1 degraded more rapidly than the other samples because owing to Nb dissolution, the surface or bulk structure of the cathode materials collapsed more rapidly for this sample than it did for the other cathode material samples. By combining this finding with the XRD results, we found that the Li_3NbO_4 layer was able to substantially mitigate side reactions from occurring with the electrolyte in the Nb-3 sample. We anticipate that using a Li_3NbO_4 layer with a higher Li^+ ionic conductor on the surface of cathode materials will promote Li^+ ions to migrate between a cathode's surface and the electrolyte interface; this would result in Li_3NbO_4 not only functioning as a protective layer but also contributing

toward reducing the amount of inactive Li^+ ions that are able to return to the cathode materials and suppressing the structural changes accompanying the Li^+ deficiency [37,38].

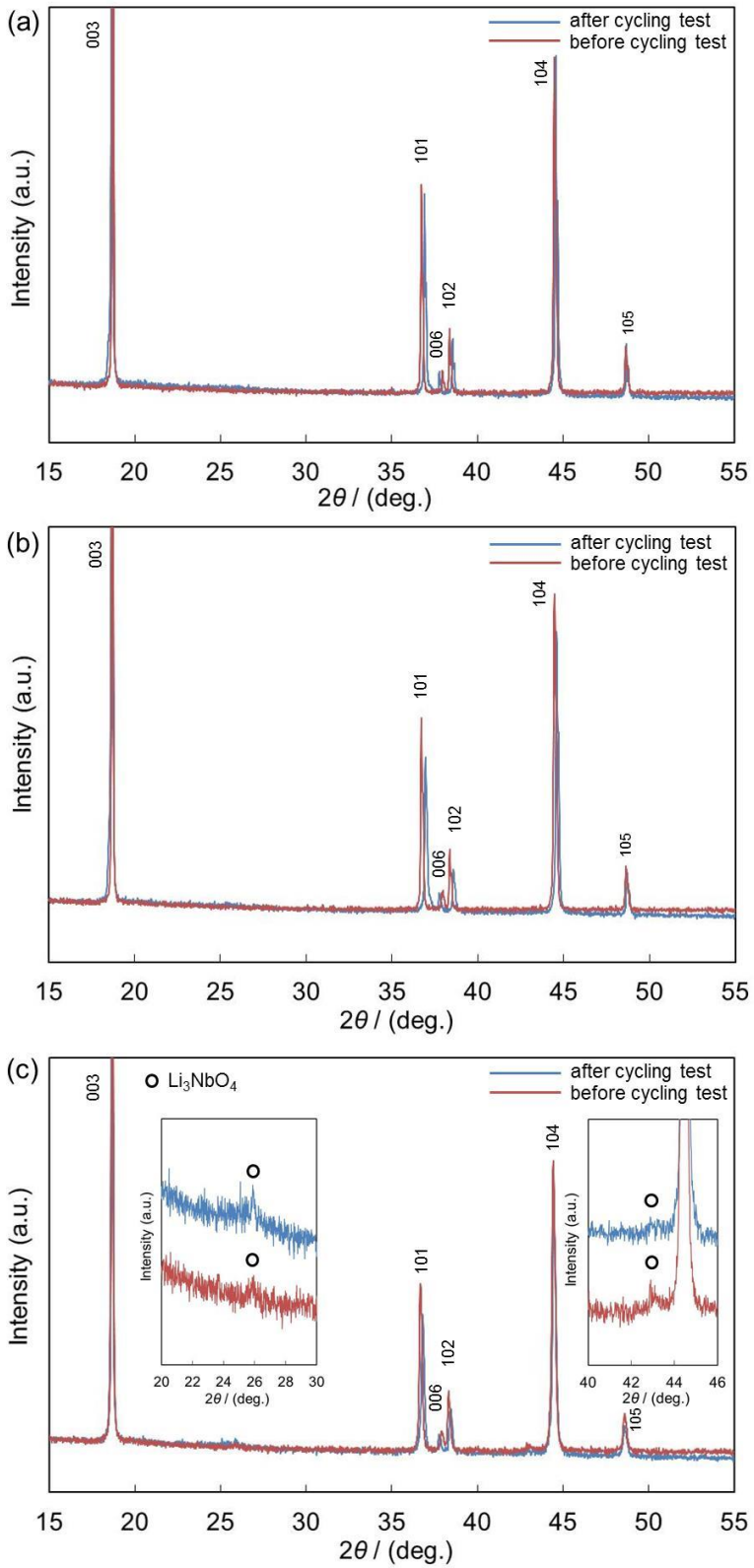

Figure 6. XRD patterns of (a) Nb-0, (b) Nb-1, and (c) Nb-3 before and after the cycling tests.

Our results therefore indicate that co-modification of the bulk structure and surface of cathode materials using Nb is a very effective method for improving the cycling performance of a cathode. Several previous studies have also found that co-modification of the bulk structure and surface of a cathode material is effective in improving the electrochemical performance of the cathode. For example, D. Wang *et al.* [26] reported on $LiNi_{0.5}Co_{0.2}Mn_{0.3}O_2$ cathode materials that had been subjected to Zr substitution and a surface polypyrrole coating; these materials were subsequently found to have good cycling stability and rate performance. Z. Wang *et al.* [39] reported that using Mg doping and a zirconium oxyfluoride (ZrO_xF_y) coating for $LiCoO_2$ (LCO) improved its cycling stability; they suggested that Mg doping was able to stabilize the crystal structure of LCO and the ZrO_xF_y coating, which means that the cathode materials could be ably protected against attacks by HF in the electrolyte. Their finding indicates that it is possible to derive performances that are superior to those produced by a single effect by combining the advantages afforded by both doping and surface coating. Our results are similar to the ones reported in these studies. In the present study, we demonstrated that by combining Nb doping, which we found to be effective for improving the thermal stability of a cathode, and Li_3NbO_4 surface modification, which we found to be effective for improving the cycling performance, the thermal stability and cycling performance of cathode materials can be simultaneously improved.

Table 2. Ratio of residual metals in the cathode materials after the cycling tests.

Sample	Ni (%)	Co (%)	Mn (%)	Nb (%)
Nb-0	99.8	99.9	99.8	-
Nb-1	99.7	99.9	99.7	67.5
Nb-3	99.8	99.9	99.8	85.6

4. CONCLUSIONS

We prepared Nb-doped and Li_3NbO_4 surface-modified NCM622 cathodes using only a solid-phase reaction. This simple technique can accommodate the industrial upscaling associated with the production of cathodic materials. We confirmed that doping the crystal structure with Nb and modifying the surface with Li_3NbO_4 were effective ways for improving a Ni-rich cathode's thermal stability and cycling performance, respectively. The amount of O_2 released from an Nb-doped NCM622 (Nb-1) cathode material was less than that released by an undoped NCM622 (Nb-0). Our results indicate that Nb doping is an effective method for improving this cathode's thermal stability. However, the cycling performance of Nb-1 was worse than that of Nb-0 possibly because the Nb in the crystal structure of Nb-1 specifically reacted with HF and the surface/bulk structure subsequently collapsed owing to Nb dissolution. Conversely, the Nb-doped, Li_3NbO_4 surface-modified NCM622 (Nb-3) exhibited an excellent cycling performance because Li_3NbO_4 has high chemical stability and

Li^+ ion conductivity protects undesirable side reactions with the electrolyte. The modification of the bulk and surface structures of NCM622 through the use of Nb simultaneously improved both the thermal stability and cycling performance of the cathode materials. These findings are very useful for engineers and scientists who aim to design advanced cathodic materials.

References

1. J. B. Goodenough, *J. Power Sources*, 174 (2007) 996.
2. J. B. Goodenough, Y. Kim, *Chem. Mater.*, 22 (2010) 587.
3. P. Miller, *Johnson Matthey Technol. Rev.*, 59 (2015) 4.
4. L. W. Liang, Z. Peng, Y. Cao, J. Duan, J. Jiang, G. Hu, *Electrochim. Acta*, 130 (2014) 82.
5. C. Demlas, M. Ménétrier, L. Croguennec, I. Saadoune, A. Rougier, C. Pouillerie, G. Prado, M. Grünea, L. Fournès, *Electrochim. Acta*, 45 (1999) 243.
6. K. Kang, G. Ceder, *Phys. Rev. B*, 74 (2006) 094105.
7. Y. Wang, J. Jiang, J. R. Dahn, *Electrochem. Commun.*, 9 (2007) 2534.
8. Y. Iriyama, H. Kurita, I. Yamada, T. Abe, Z. Ogumi, *J. Power Sources*, 137 (2004) 111.
9. W. Cho, S. M. Kim, J. H. Song, T. Yim, S. G. Woo, K. W. Lee, J. S. Kim, Y. J. Kim, *J. Power Sources*, 282 (2015) 45.
10. K. Araki, N. Taguchi, H. Sakaebe, K. Tatsumi, Z. Ogumi, *J. Power Sources*, 269 (2014) 236.
11. Y. Chen, Y. Zhang, B. Chen, Z. Wang, C. Lu, *J. Power Sources*, 256 (2014) 20.
12. G. R. Hu, X. R. Deng, Z. D. Peng, K. Du, *Electrochim. Acta*, 53 (2008) 2567.
13. S. -U. Woo, C. S. Yoon, K. Amine, I. Belharouak, Y. -K. Sun, *J. Electrochem. Soc.*, 154 (2007) A1005.
14. H. W. Chan, J. G. Duh, S. R. Sheen, *Electrochim. Acta*, 51 (2006) 3645.
15. J. He, X. Chu, Y. B. He, D. Liu, Y. Liu, J. Wu, B. Li, F. Kang, *Int. J. Electrochem. Sci.*, 11 (2016) 6902.
16. F. Wu, J. Tian, Y. Su, Y. Guan, Y. Jin, Z. Wang, T. He, L. Bao, S. Chen, *J. Power Sources*, 269 (2014) 747.
17. H. Liu, J. Li, Z. Zhang, Z. Gong, Y. Yang, *Electrochim. Acta*, 49 (2004) 1151.
18. K. K. Lee, W. S. Yoon, K. B. Kim, K. Y. Lee, S. T. Hong, *J. Power Sources*, 97–98 (2001) 308.
19. J. Y. Liao, A. Manthiram, *J. Power Sources*, 282 (2015) 429.
20. H. Konishi, M. Yoshikawa, T. Hirano, *J. Power Sources*, 244 (2013) 23.
21. H. P. Loock, B. Simard, *J. Chem. Phys.*, 109 (1998) 8980.
22. J. A. Dean, Lange's Handbook of Chemistry, fifteenth ed., McGraw Hill, (1998) New York, U.S.
23. W. Sun, M. Xie, X. Shi, L. Zhang, *Mater. Res. Bull.*, 61 (2015) 287.
24. Y. Zhang, E. Zhou, D. Song, X. Shi, X. Wang, J. Guo, L. Zhang, *Phys. Chem. Chem. Phys.*, 16 (2014) 17792.
25. M. Mladenov, R. Stoyanova, E. Zhecheva, S. Vassilev, *Electrochem. Commun.*, 3 (2001) 410.
26. D. Wang, X. Li, Z. Wang, H. Guo, Y. Xu, Y. Fan, *Electrochim. Acta*, 196 (2016) 101.
27. R. D. Shannon, *Acta Cryst.*, A32 (1976) 751.
28. S. Yang, X. Wang, X. Yang, L. Liu, Z. Liu, Y. Bai, Y. Wang, *J. Solid State Electrochem.*, 16 (2012) 1229.
29. S. M. Bak, K. W. Nam, W. Chang, X. Yu, E. Hu, S. Hwang, E. A. Stach, K. B. Kim, K. Y. Chung, X. Q. Yang, *Chem. Mater.*, 25 (2013) 337.
30. M. Guilmard, L. Croguennec, D. Denux, C. Delmas, *Chem. Mater.*, 15 (2003) 4476.
31. Z. Yang, W. Xiang, Z. Wu, F. He, J. Zhang, Y. Xiao, B. Zhong, X. Guo, *Ceramics Int.*, 43 (2017) 3866.
32. S. K. Martha, J. Nanda, G. M. Veith, N. J. Dudney, *J. Power Sources*, 199 (2012) 220.

33. R. Amine, H. H. Sun, H. J. Sun, J. Prakash, *Electrochem. Solid-State Lett.*, 13 (2010) A101.
34. H. R. Kim, S. G. Woo, J. H. Kim, W. Cho, Y. J. Kim, *J. Electroanal. Chem.*, 782 (2016) 168.
35. J. Yang, Y. Xia, *J. Electrochem. Soc.*, 163 (2016) A2665.
36. J. Li, L. Wang, Q. Zhang, X. He, *J. Power Sources*, 190 (2009) 149.
37. N. Y. Kim, T. Yim, J. H. Song, J. S. Yu, Z. Lee, *J. Power Sources*, 307 (2016) 641.
38. D. P. Abraham, R. D. Twesten, M Balasubramanian, I Petrov, J McBreen, K Amine, *Electrochem. Commun.*, 4 (2002) 620.
39. Z. Wang, Z. Wang, H. Guo, W. Peng, X. Li, *Ceramics Int.*, 41 (2015) 469.